Electronic Supplementary Information (ESI)

Cationic Zr-based metal organic framework with enhanced acidic resistance for selective and efficient removal of CrO_4^{2-}

Chao Jiang[a], Ruopei Sun[a], Ziyao Du[a], Vikramjeet Singh[c] and Suwen Chen[ab]*

[a]Radiochemistry Lab, School of Nuclear Science and Technology, Lanzhou University, 730000, Lanzhou, P. R. China

[b]Key Laboratory of Special Function Materials and Structure Design, Ministry of Education, Lanzhou University, 730000, Lanzhou, P. R. China

[c]Nanoengineered Systems Laboratory, UCL Mechanical Engineering, University College London, London, UK

* Corresponding author: chensuwen@lzu.edu.cn

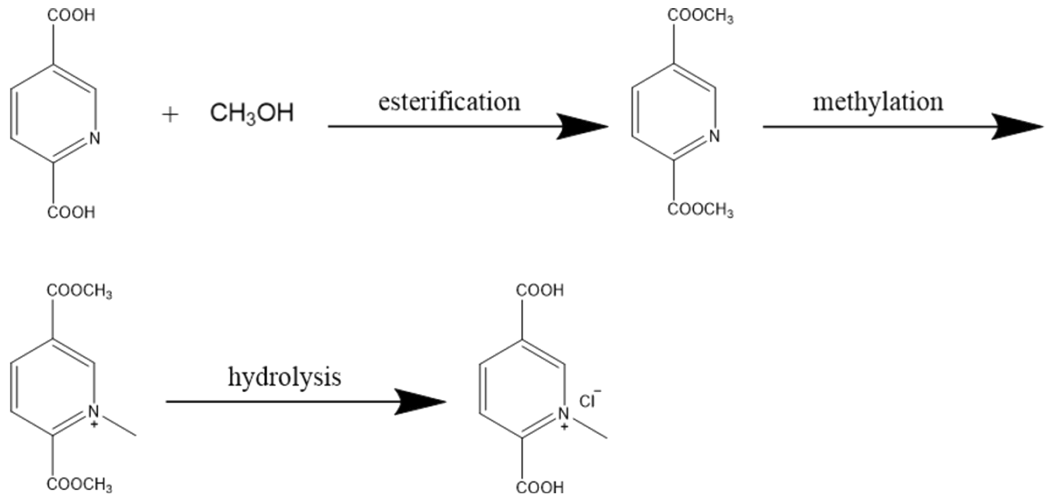

Scheme.S1. Synthesis of Ligand me-PyDC.

Table.S1. Experimental parameters for synthesis of Zr-C-MOF.

number	$ZrCl_4$ (mg)	me-PyDC (mg)	H_2O (μL)	formic acid (μL)	Product	Yield (mg)
1	26.5	25.0	4960	40	white power	25.1
2	26.5	25.0	4920	80	white power	24.1
3	26.5	25.0	4840	160	white power	27.1
4	26.5	25.0	4500	500	white power	20.8
5	26.5	25.0	4000	1000	white power	20.9
6	26.5	25.0	3000	2000	white power	3.7
7	26.5	25.0	2000	3000	no solid	0

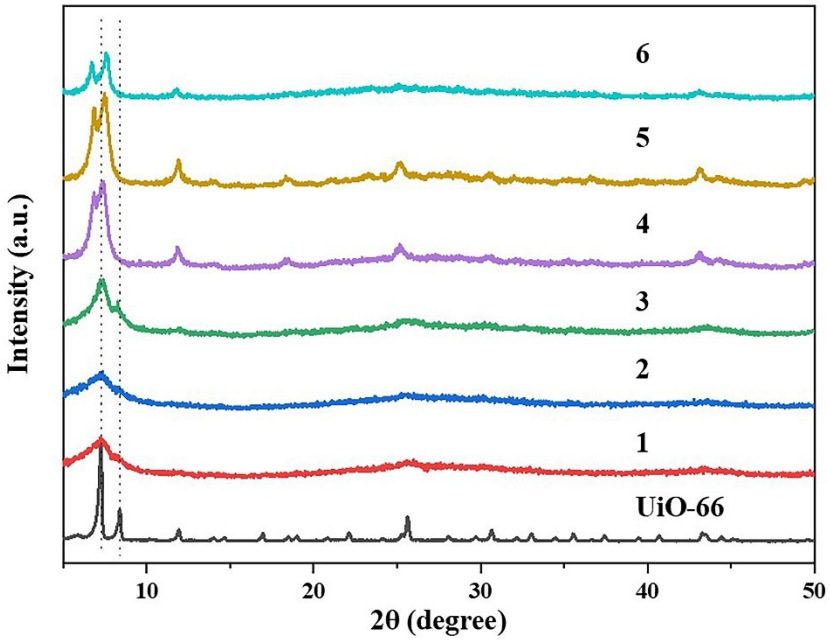

Fig.S1. Powder X-ray diffraction (PXRD) patterns of UiO-66 and product synthesized at different experimental parameters.

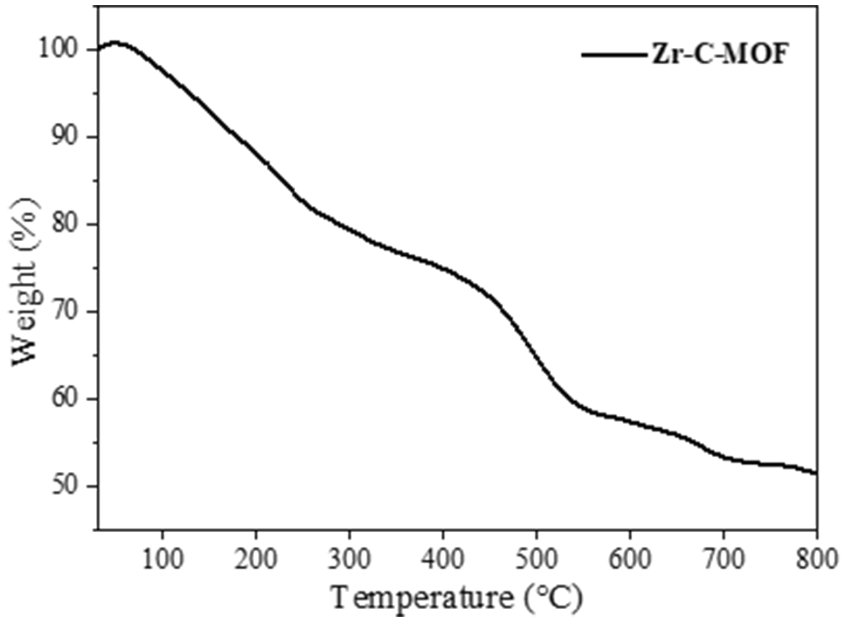

Fig.S2. TGA curves of Zr-C-MOF.

Table.S2. Elemental analysis of Zr-C-MOF.

Sample	C %	H %	N %
Zr-C-MOF	20.6	2.460	2.59

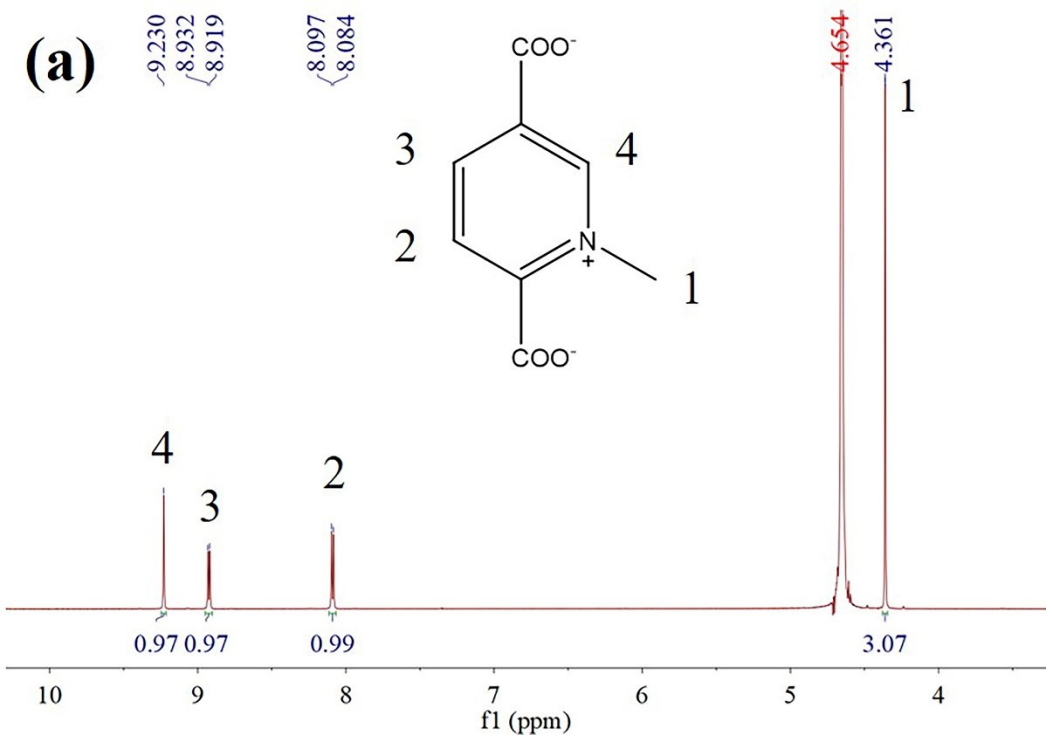
(a)
9.230
8.932
8.919
8.097
8.084
4.654
4.361
COO⁻
COO⁻
N
+
1
2
3
4
0.97 0.97
0.99
3.07
10
9
8
7
6
5
4
f1 (ppm)

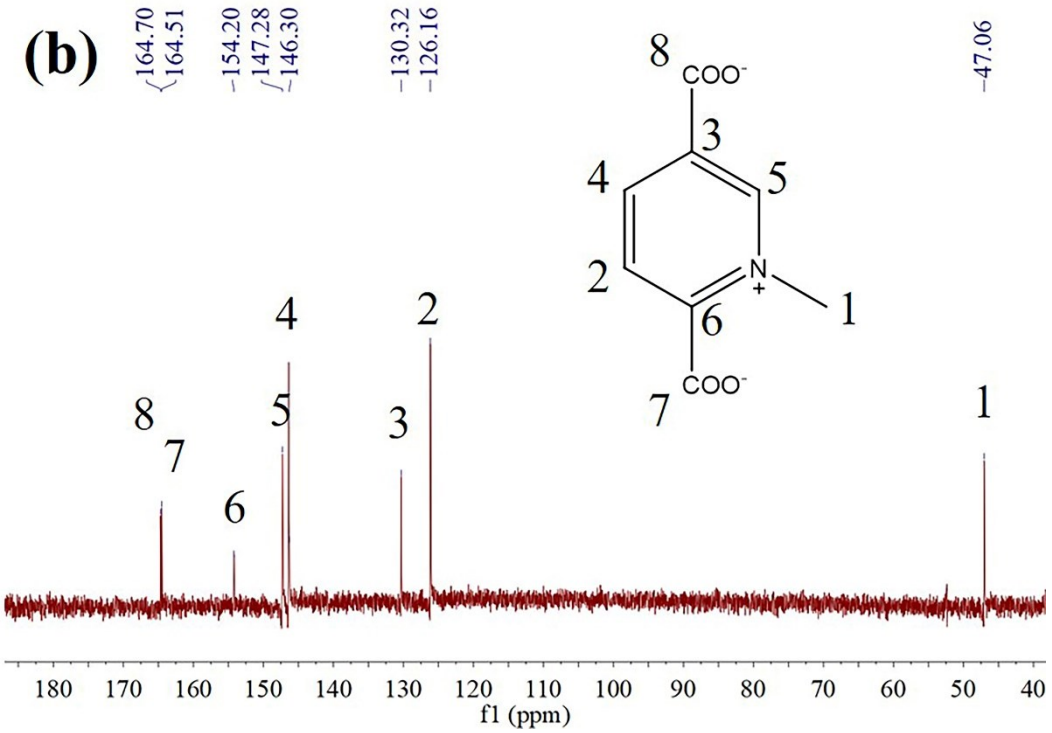
(b)
164.70
164.51
154.20
147.28
146.30
130.32
126.16
47.06
8
COO⁻
3
4
5
2
N
+
1
6
7
COO⁻
180
170
160
150
140
130
120
110
100
90
80
70
60
50
40
f1 (ppm)

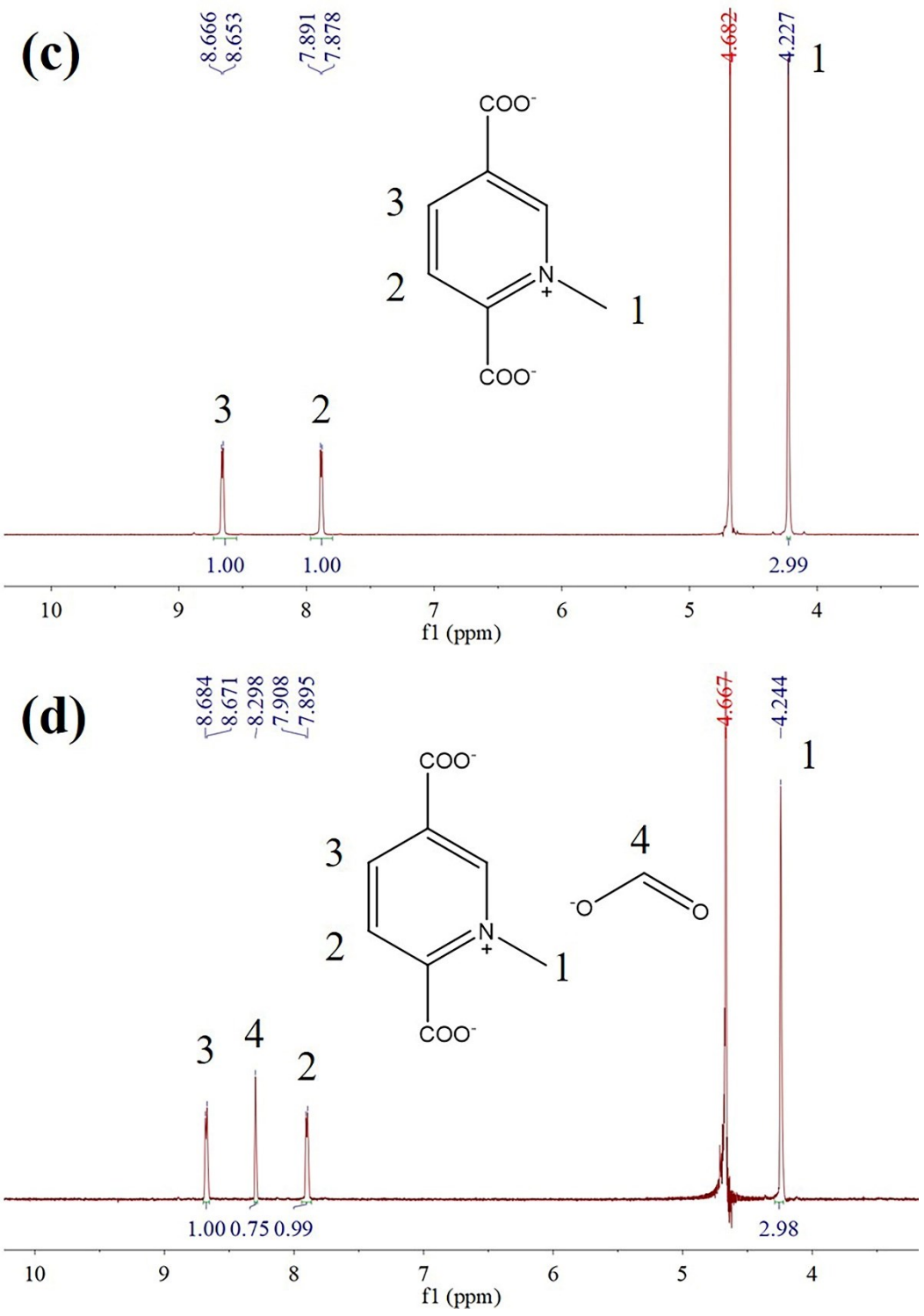

Fig.S3. 600 MHz ^{1}H-NMR, and 150 MHz ^{13}C-NMR spectra. **(a)**^{1}H-NMR of me-PyDC (D_2O), δ=9.23 (s, 1H), 8.92 (d, J=7.8 Hz, 1H), 8.09 (d, J=7.8 Hz, 1H), 4.36 ppm (s, 3H). **(b)**^{13}C-NMR of me-PyDC (D_2O), δ=164.7, 164.5, 154.2, 147.3, 146.3, 130.3, 126.2, 47.1 ppm. **(c)**^{1}H-NMR of me-PyDC in 0.5 M KOH/D_2O, δ=8.66 (d, J=7.8 Hz, 1H), 7.88 (d, J=7.8 Hz, 1H), 4.23 ppm (s, 3H). **(d)**^{1}H-NMR of Zr-C-MOF digested in

0.5 M KOH/D_2O, δ=8.67 (d, J=7.8 Hz, 1H), 8.30 (s, 0.75H, H atom from formate), 7.90 (d, J=7.8 Hz, 1H), 4.24 ppm (s, 3H).

Note: Absence of H peak at 9.2 ppm in (c) and (d) compared with (a) was due to deuterium exchange induced by proximity to N-methyl group in alkaline solution

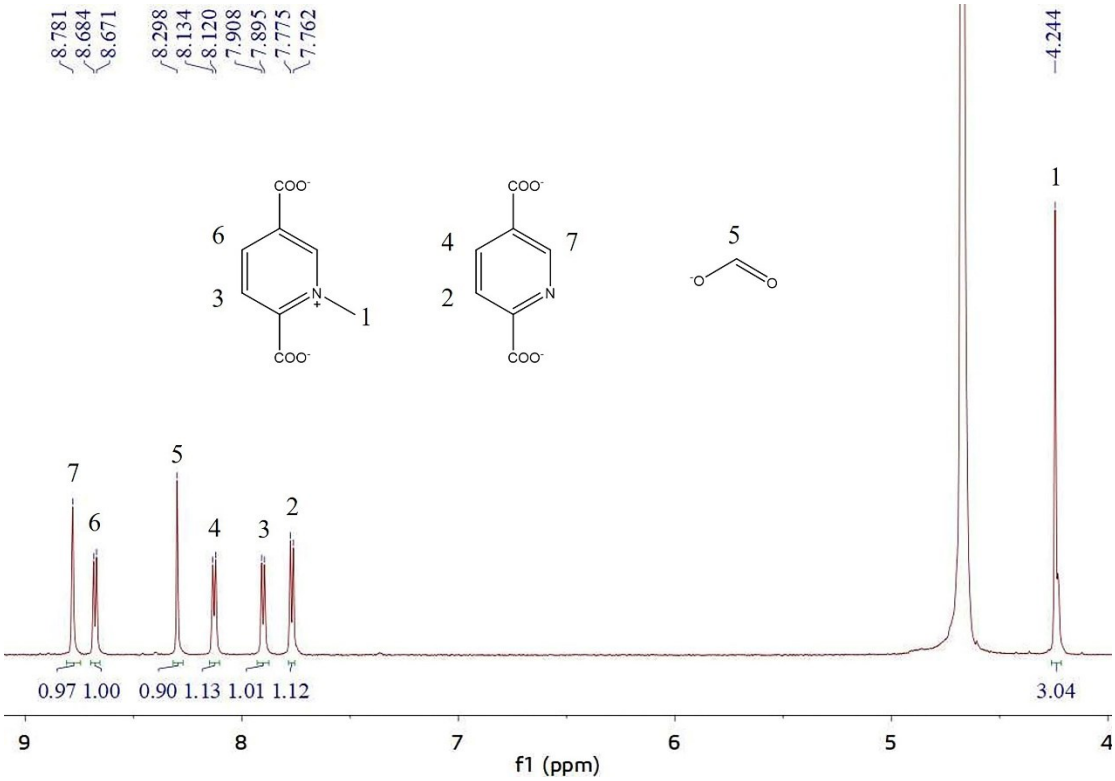

Fig.S4. 600 MHz ^{1}H-NMR spectra. ^{1}H-NMR of UiO-66-me-PyDC digested in 0.5 M KOH/D_2O, δ=8.78 (s, 1H), 8.68 (d, J=7.8 Hz, 1H), 8.30 (s, 0.9H), 8.13 (d, J=7.8 Hz, 1.13 H), 7.90 (d, 7.8 Hz, 1H), 7.77 (d, 7.8 Hz, 1.12H), 4.24 (s, 3H).

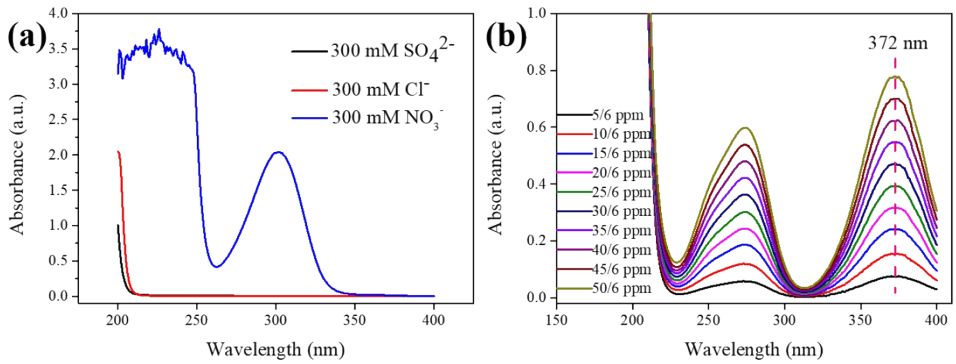

Fig.S5. UV-visible spectrum of **(a)** 300mol·L^{-1} Cl^-, NO_3^-, SO_4^{2-} **(b)** CrO_4^{2-}.

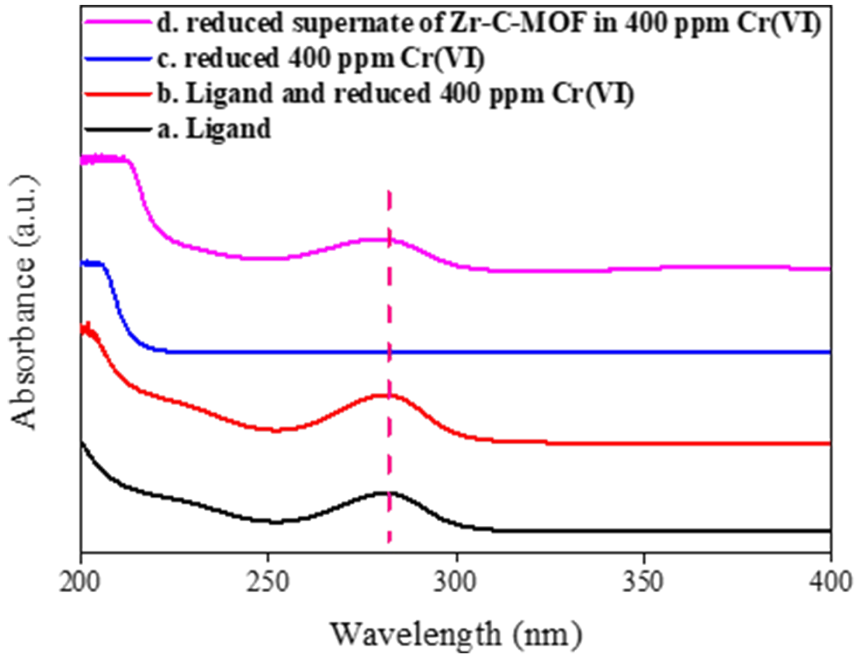

Fig.S6. UV-visible spectrum of **(a)** me-PyDC in water **(b)** me-PyDC and 400 ppm CrO_4^{2-} reduced by $FeCl_2$**(c)** 400 ppm CrO_4^{2-} reduced by $FeCl_2$**(d)** supernatant after adsorption by Zr-C-MOF in 400 ppm CrO_4^{2-} and further reduced by $FeCl_2$. To avoid the peak of CrO_4^{2-} at 275 nm covering the peak of ligand, CrO_4^{2-} was reduced by $FeCl_2$. All samples above were adjusted to pH=12, and centrifuged to afford clear solutions.

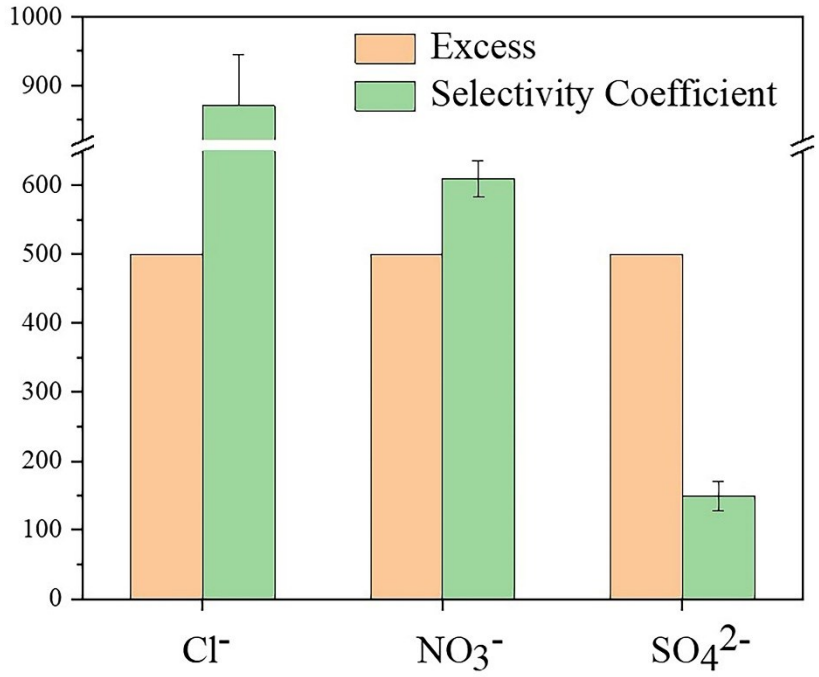

Fig.S7. Selectivity coefficient of Zr-C-MOF for Cr (VI) over other anion at 500-times excess.

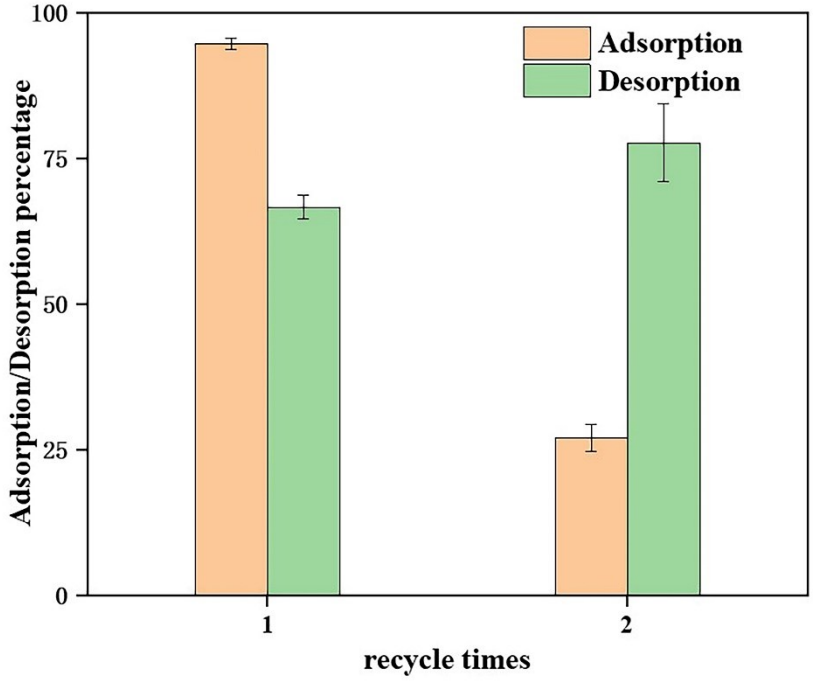

Fig.S8. Adsorption-Desorption experiment of cycling experiment

Table.S3. Fitting results based on the Pseudo-first-order kinetic and Pseudo-second-order kinetic models.

Sample	Pseudo-first-order kinetic model			Pseudo-second-order kinetic model		
	q_e (mg g^{-1})	k_1 (min^{-1})	R^2	q_e (mg g^{-1})	k_2 (g mg^{-1} min^{-1})	R^2
Zr-C-MOF	49.49	13.46	0.78	49.65	9.20	＞0.99

Table.S4. Fitting results based on the Langmuir and Freundlich models.

Sample	Langmuir			Freundlich		
	q_m ($mg \cdot g^{-1}$)	K_L ($L \cdot mg^{-1}$)	R^2	k_F ($mg \cdot g^{-1}$)	n	R^2
Zr-C-MOF	83.3	0.923	＞0.99	23.7	2.41	0.69

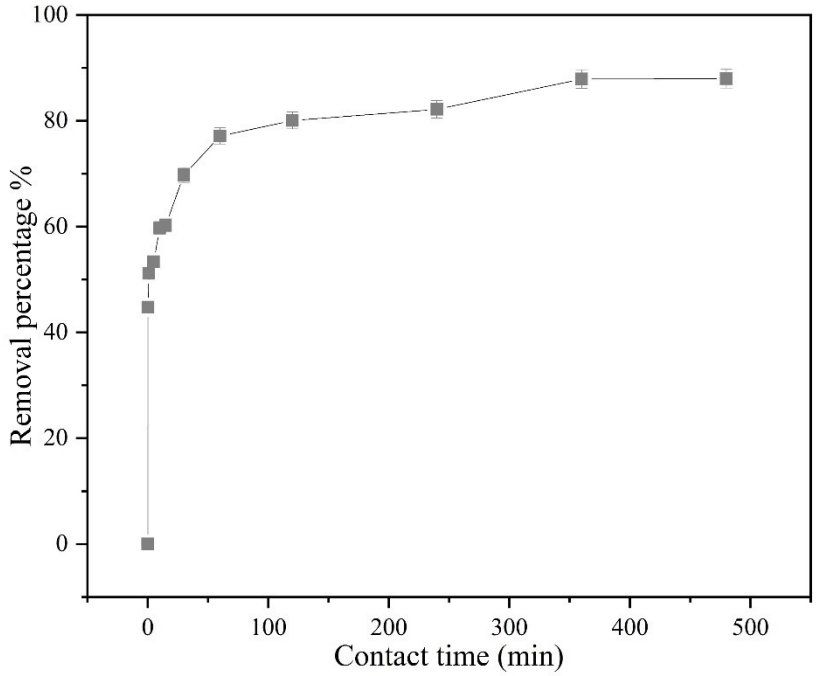

Fig.S9. Sorption kinetics of CrO_4^{2-} by UiO-66-me-PyDC

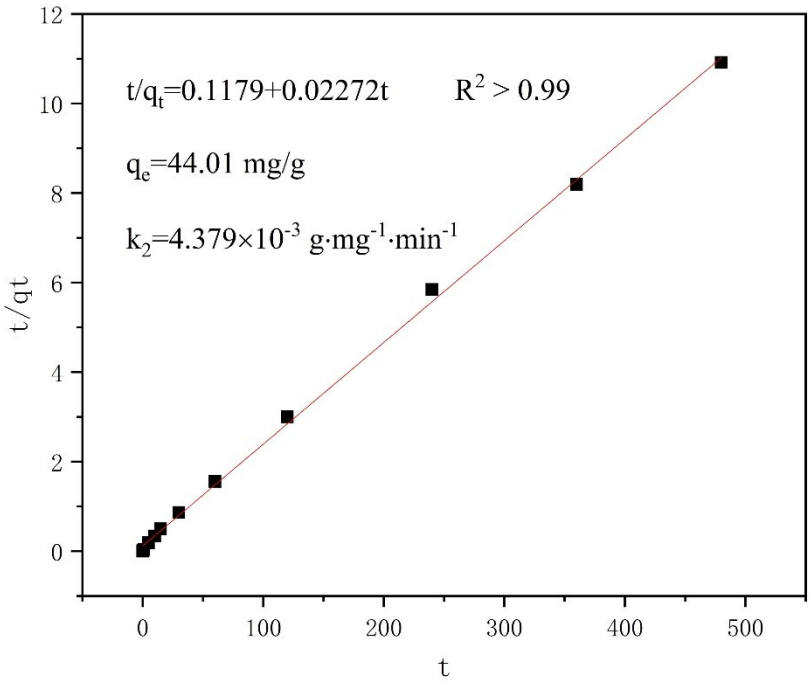

Fig.S10. Fitting results of UiO-66-me-PyDC based on the Pseudo-second-order kinetic models.

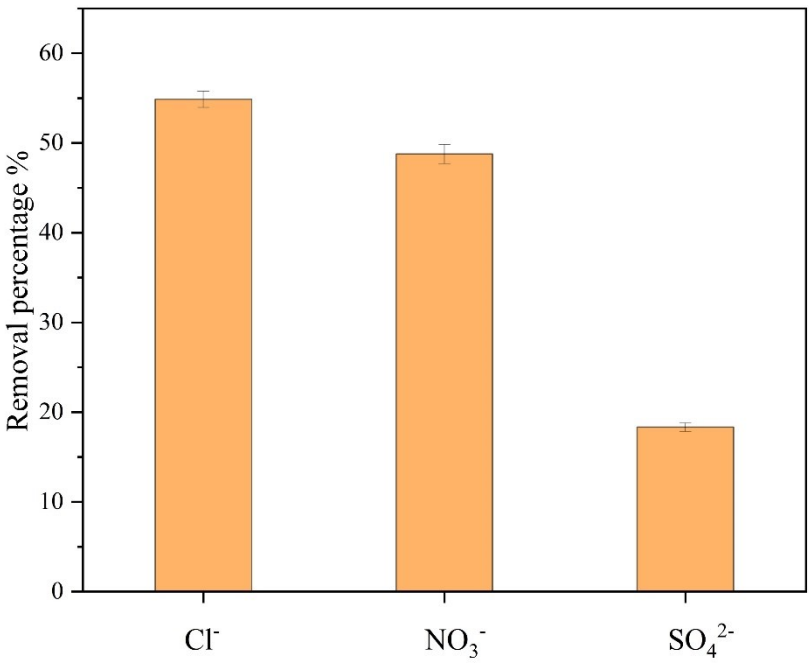

Fig.S11. Effect of 500-fold competing anions on the adsorption of CrO_4^{2-} by UiO-66-me-PyDC.

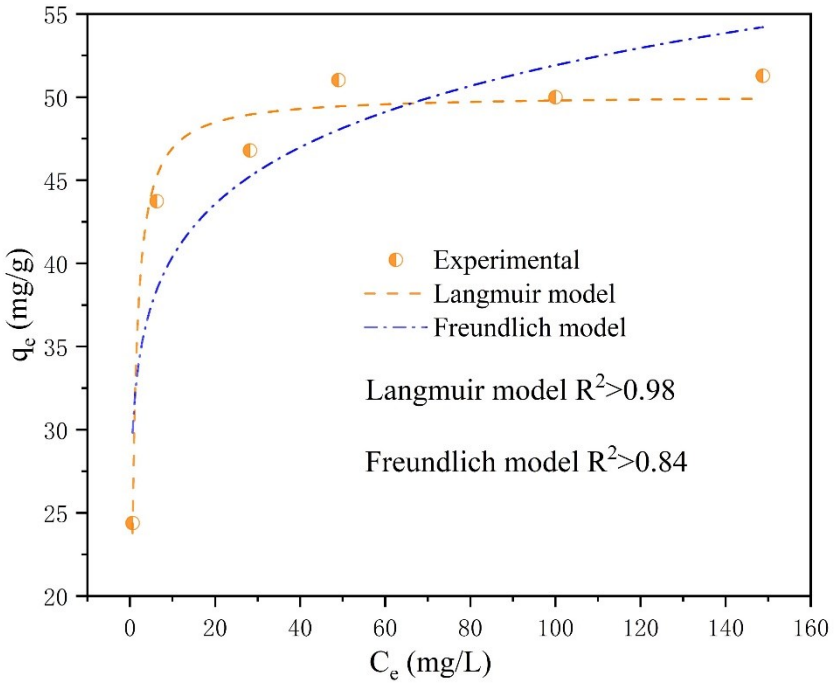

Fig.S12. Adsorption isotherm of CrO_4^{2-} on UiO-66-me-PyDC.